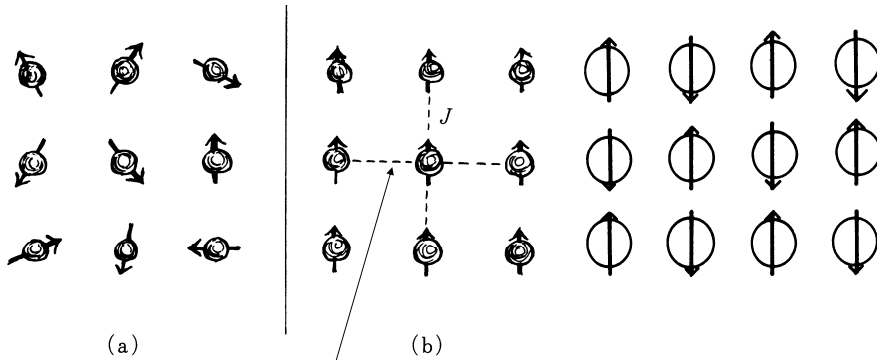


Introduction to Magnetism

Paramagnetism

Ferromagnetism

Antiferromagnetism



Exchange interaction

Hamiltonian in Magnetic Substances

$$H = -2J \sum_{ij} \mathbf{S}_i \cdot \mathbf{S}_j$$

$J < 0$ (in case of wave functions mixed)

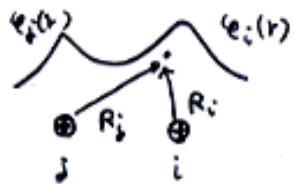
: Antiferromagnetism

$J > 0$ (in case of wave functions being orthogonalized)

: Ferromagnetism

Model Hamiltonian for Strongly Correlated Electrons Systems

$$-t_{ij} = \int \psi_j^\dagger(\mathbf{r}) \left[-\frac{\hbar^2 \nabla^2}{2m} - \frac{e^2}{R_i} - \frac{e^2}{R_j} \right] \psi_i(\mathbf{r}) d\mathbf{r}$$



U : Coulomb repulsion

t : Transferred integral

$$\mathcal{H} = - \sum_{ij\sigma} t_{ij} a_{i\sigma}^\dagger a_{j\sigma} + U \sum_{i,\sigma} n_{i\sigma} \cdot n_{i,-\sigma}$$

$$- 2J \sum_{ij} \mathbf{S}_i \cdot \mathbf{S}_j$$

(6-2) In order to improve the HL wave function;

$$\Phi_{HL} = \frac{1}{\sqrt{2(1+S^2)}} [\psi_a(1)\psi_b(2) + \psi_b(1)\psi_a(2)]$$

We incorporate the following states, using $\psi_a(1)\psi_a(2)$ and $\psi_b(1)\psi_b(2)$

$$\Phi' = \frac{1}{\sqrt{2}} [\psi_a(1)\psi_a(2) + \psi_b(1)\psi_b(2)]$$

Then, the improved trial wave function is expressed by $\Phi = c_1 \Phi_{HL} + c_2 \Phi'$.

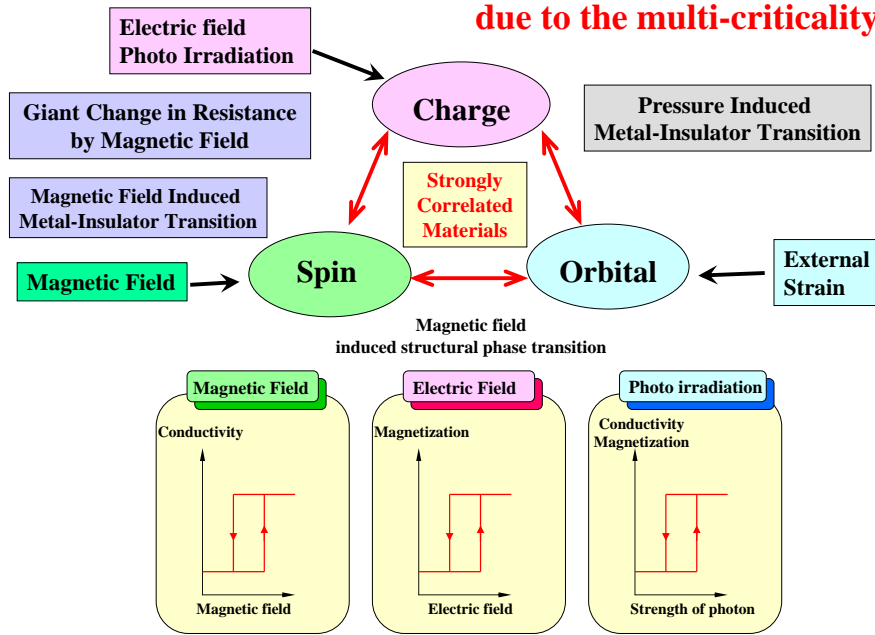
Show how to get the following relation and solve an eigen energy for this state

$$\begin{vmatrix} 2\varepsilon + U_1 + J' - E & 2t \\ 2t & 2\varepsilon + U_0 + J' - E \end{vmatrix} = 0$$

If $U_0 - U_1 \gg |t|$ is valid for Mott insulator, show that the eigen energy is given as the follow;

$$E_{HL} = 2\varepsilon + U_1 + \boxed{J' - \frac{4t^2}{U_0 - U_1}}$$

Giant Response to magnetic and electric fields due to the multi-criticality



周期表

(基底状態の中性原子の外殻電子配置)

原子およびイオンの電子配置を示す記号についてはすべての初歩的な原子物理学の教科書において述べられている。文字s, p, d...はnを単位とする軌道角モーメント0, 1, 2, ...をもっている電子を示す。文字の左側の数字は軌道の主量子数を示す。右肩上の数字はその軌道の電子数である。

H ¹																	He ²				
1s																	1s ²				
Li ³	Be ⁴															B ⁵	C ⁶	N ⁷	O ⁸	F ⁹	Ne ¹⁰
2s	2s ²															2s ² 2p	2s ² 2p ²	2s ² 2p ³	2s ² 2p ⁴	2s ² 2p ⁵	2s ² 2p ⁶
Na ¹¹	Mg ¹²															Al ¹³	Si ¹⁴	P ¹⁵	S ¹⁶	Cl ¹⁷	Ar ¹⁸
3s	3s ²															3s ² 3p	3s ² 3p ²	3s ² 3p ³	3s ² 3p ⁴	3s ² 3p ⁵	3s ² 3p ⁶
K ¹⁹	Ca ²⁰	Sc ²¹	Ti ²²	V ²³	Cr ²⁴	Mn ²⁵	Fe ²⁶	Co ²⁷	Ni ²⁸	Cu ²⁹	Zn ³⁰	Ga ³¹	Ge ³²	As ³³	Se ³⁴	Br ³⁵	Kr ³⁶				
4s	4s ²	3d	3d ²	3d ³	3d ⁴	3d ⁵	3d ⁶	3d ⁷	3d ⁸	3d ⁹	3d ¹⁰	4s ² 4p	4s ² 4p ²	4s ² 4p ³	4s ² 4p ⁴	4s ² 4p ⁵	4s ² 4p ⁶				
Rb ³⁷	Sr ³⁸	Y ³⁹	Zr ⁴⁰	Nb ⁴¹	Mo ⁴²	Tc ⁴³	Ru ⁴⁴	Rh ⁴⁵	Pd ⁴⁶	Ag ⁴⁷	Cd ⁴⁸	In ⁴⁹	Sn ⁵⁰	Sb ⁵¹	Te ⁵²	I ⁵³	Xe ⁵⁴				
5s	5s ²	4d	4d ²	4d ³	4d ⁴	4d ⁵	4d ⁶	4d ⁷	4d ⁸	4d ⁹	4d ¹⁰	5s ² 5p	5s ² 5p ²	5s ² 5p ³	5s ² 5p ⁴	5s ² 5p ⁵	5s ² 5p ⁶				
Cs ⁵⁵	Ba ⁵⁶	La ⁵⁷	Hf ⁷²	Ta ⁷³	W ⁷⁴	Re ⁷⁵	Os ⁷⁶	Ir ⁷⁷	Pt ⁷⁸	Au ⁷⁹	Hg ⁸⁰	Tl ⁸¹	Pb ⁸²	Bi ⁸³	Po ⁸⁴	At ⁸⁵	Rn ⁸⁶				
6s	6s ²	5d	4f ¹⁴	5d ²	5d ³	5d ⁴	5d ⁵	5d ⁶	5d ⁷	5d ⁸	5d ⁹	6s ² 6p	6s ² 6p ²	6s ² 6p ³	6s ² 6p ⁴	6s ² 6p ⁵	6s ² 6p ⁶				
Fr ⁸⁷	Ra ⁸⁸	Ac ⁸⁹																			
7s	7s ²	6d	7s ²																		
			Ce ⁵⁸	Pr ⁵⁹	Nd ⁶⁰	Pm ⁶¹	Sm ⁶²	Eu ⁶³	Gd ⁶⁴	Tb ⁶⁵	Dy ⁶⁶	Ho ⁶⁷	Er ⁶⁸	Tm ⁶⁹	Yb ⁷⁰	Lu ⁷¹					
			4f ²	4f ³	4f ⁴	4f ⁵	4f ⁶	4f ⁷	4f ⁷	4f ⁸	4f ⁹	4f ¹⁰	4f ¹¹	4f ¹²	4f ¹³	4f ¹⁴					
			6s ²	6s ²	6s ²	6s ²	6s ²	6s ²	6s ²	6s ²	6s ²	6s ²	6s ²	6s ²	6s ²	6s ²					
			Th ⁹⁰	Pa ⁹¹	U ⁹²	Np ⁹³	Pu ⁹⁴	Am ⁹⁵	Cm ⁹⁶	Bk ⁹⁷	Cf ⁹⁸	Es ⁹⁹	Fm ¹⁰⁰	Md ¹⁰¹	No ¹⁰²	Lr ¹⁰³					
			6d ²	6d ²	6d ²	7s ²	7s ²	7s ²	7s ²	7s ²	7s ²	7s ²	7s ²	7s ²	7s ²	7s ²					

3d 遷移磁性元素

4f 希土類磁性元素

$$H_{\text{eff}} = \sum_i \zeta l_i \cdot S/n = \zeta/n(\sum_i l_i) \cdot S = (\zeta/n)L \cdot S$$

$$\lambda = \zeta/n > 0$$

$$n > 2l+1 : \lambda = -\zeta/(4l+2-n) < 0$$

$$n = 2l+1 : L=0, S=(2l+1)/2 \rightarrow H_{\text{eff}}=0$$

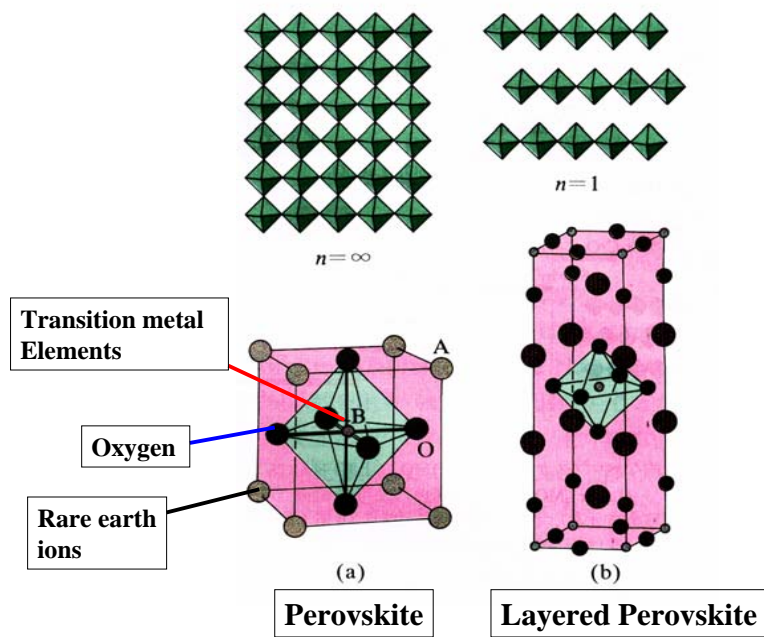
表 2-3 スピン軌道相互作用の定数

	電子数	電子状態	$\lambda \text{ cm}^{-1}$
Ti ³⁺	d ¹	² D	154
V ³⁺	d ²	³ F	104
Cr ³⁺	d ³	⁴ F	87
Mn ³⁺	d ⁴	⁵ D	85
V ²⁺	d ³	⁴ F	55
Cr ²⁺	d ⁴	⁵ D	57
Fe ²⁺	d ⁶	⁶ D	-100
Co ²⁺	d ⁷	⁴ F	-180
Ni ²⁺	d ⁸	³ F	-335
Cu ²⁺	d ⁹	² D	-828

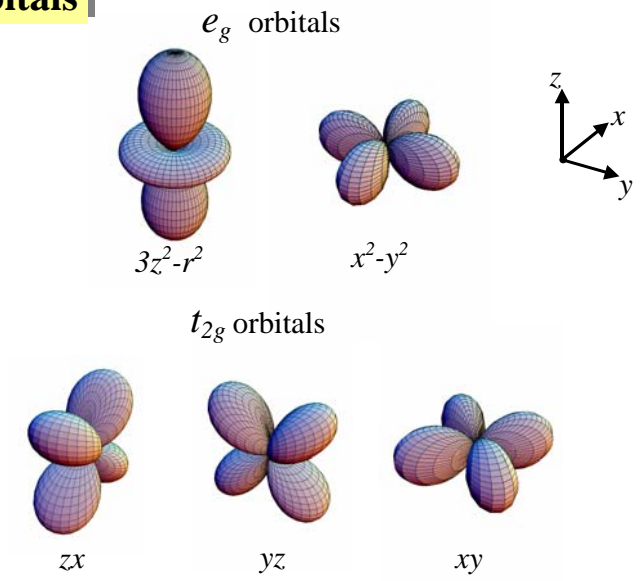
Electron Configuration in Transition Metal Ions

	d ¹	d ²	d ³	d ⁴	d ⁵	d ⁶	d ⁷	d ⁸	d ⁹
	Ti ³⁺	V ³⁺	Cr ³⁺	Mn ³⁺	Fe ³⁺	Co ³⁺	Ni ³⁺	Cu ³⁺	
	V ⁴⁺	Cr ⁴⁺	Mn ⁴⁺	Fe ⁴⁺					
e _g	↑	↑↑	↑↑↑	↑↑↑↑	↑↑↑↑↓	↑↑↑↑↓↑	↑↑↑↑↓↑↓	↑↑↑↑↓↑↓↑	↑↑↑↑↓↑↓↑↓
t _{2g}	↑↑↑	↑↑↑↑	↑↑↑↑↑	↑↑↑↑↑↓	↑↑↑↑↑↓↑	↑↑↑↑↑↓↑↓	↑↑↑↑↑↓↑↓↑	↑↑↑↑↑↓↑↓↑↓	↑↑↑↑↑↓↑↓↑↓↑
	S=1/2	S=1	S=3/2	S=2	S=5/2	S=0	S=1/2	S=1	S=1/2
						↑↑	↑↑↑	↑↑↑↑	↑↑↑↑↓
						S=1	S=2		

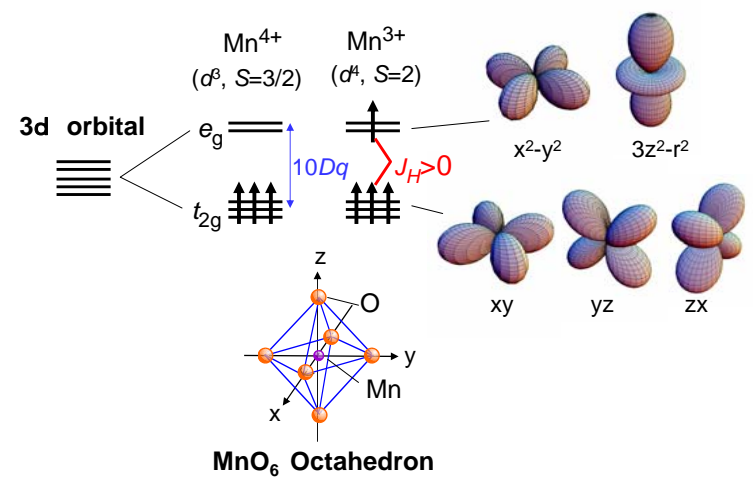
Hunds' rule and Crystal Electric Field Effect



3d orbitals



Electronic Structure of Manganese oxides



Hund's Coupling $J_H >$ CEF splitting $10Dq$

When J is negative due to the overlap of wave functions among nearest neighbor atomic sites, Spins are anti-parallel. On the other hand, if the wave function is orthogonalized, J is always positive and hence ferromagnetism is realized

Proof:

$$J_{n_1 n_2} = \int \varphi_{n_1}^*(r_1) \varphi_{n_2}^*(r_2) \frac{e^2}{r_{12}} \varphi_{n_1}(r_2) \varphi_{n_2}(r_1) d\tau_1 d\tau_2$$

$1/r$ is expanded in a Fourier series as

$$\frac{e^2}{r_{12}} = \frac{1}{V} \sum_{\mathbf{k}} \frac{4\pi e^2}{k^2} e^{i\mathbf{k} \cdot (\mathbf{r}_1 - \mathbf{r}_2)}$$

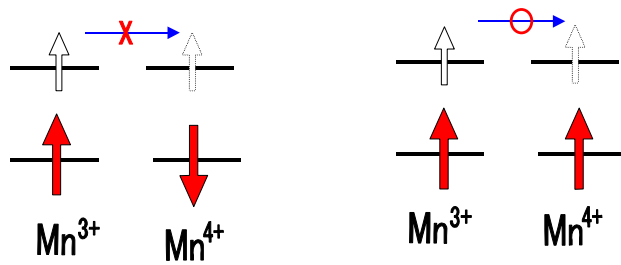
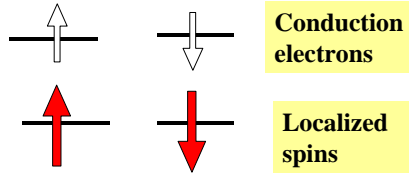
$J = -2St + J' = J'$ (because of $S=0$)

$$J_{n_1 n_2} = \frac{1}{V} \sum_{\mathbf{k}} \frac{4\pi e^2}{k^2} \int \varphi_{n_1}^*(r_1) \varphi_{n_2}(r_1) e^{i\mathbf{k} \cdot \mathbf{r}_1} d\tau_1 \times \int \varphi_{n_1}^*(r_2) \varphi_{n_2}(r_2) e^{-i\mathbf{k} \cdot \mathbf{r}_2} d\tau_2 > 0$$

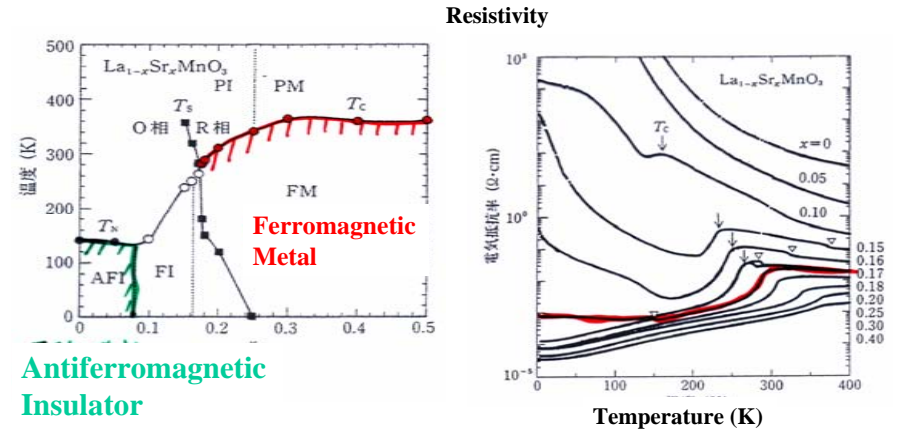
のように書きかえられる。したがって $J_{n_1 n_2}$ は常に正である。

Strong coupling of spin and charge degrees of freedom

Hund's coupling



When carriers doped, metallic state is stabilized



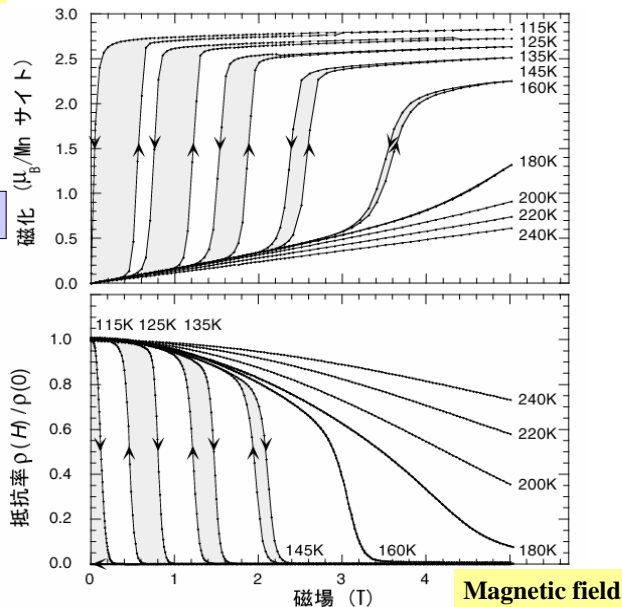
Antiferromagnetic Insulator

CMR effect

$(\text{Nd,Sm})_{0.5}\text{Sr}_{0.5}\text{MnO}_3$

Colossal Magneto Resistance

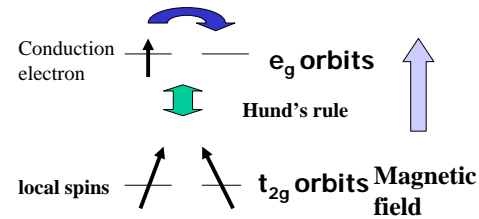
Magnetization



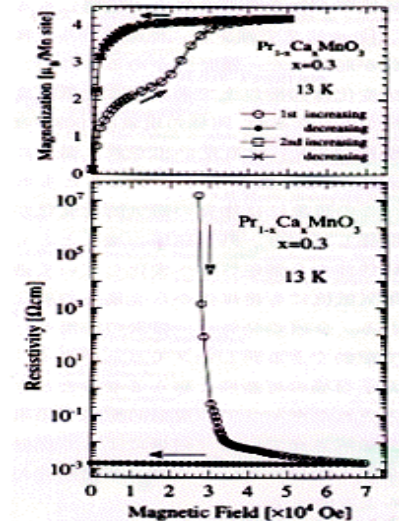
Resistance

Magnetic Field Control of Magnetic and Transport Properties in $\text{Pr}_{1-x}\text{Ca}_x\text{MnO}_3$

Competition between Ferromagnetic Metallic and charge ordered insulating phases



Conductivity controlled by Magnetic field → local spins → mobile electrons



Resistance

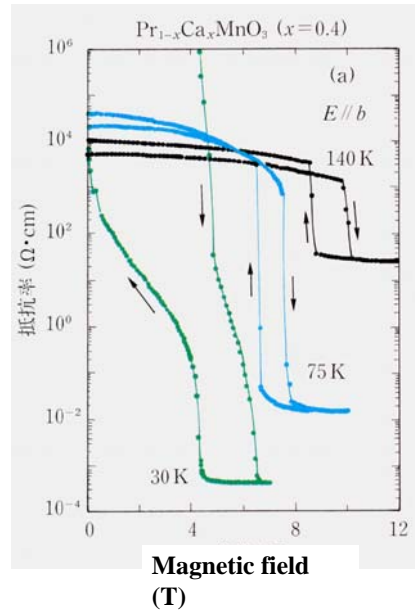
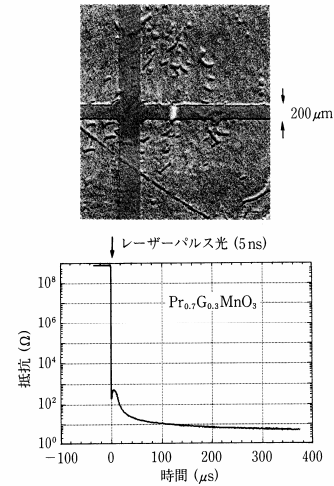
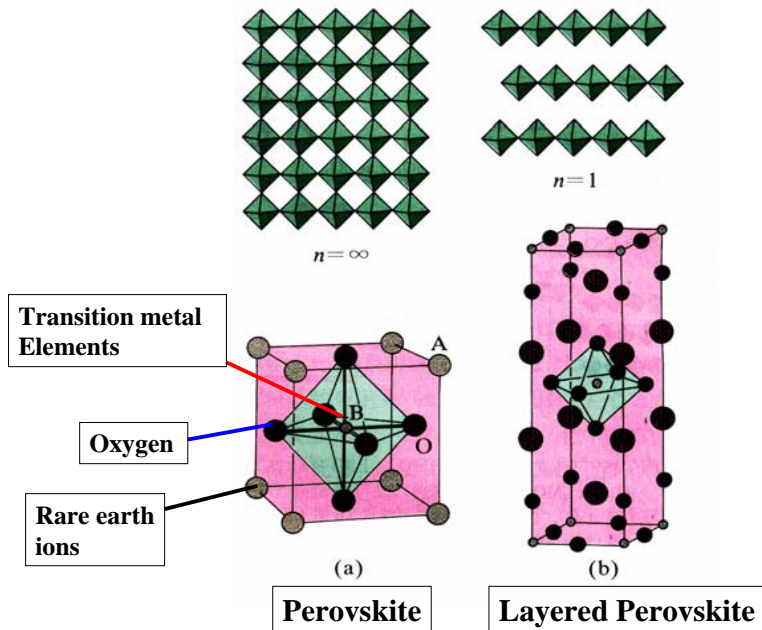
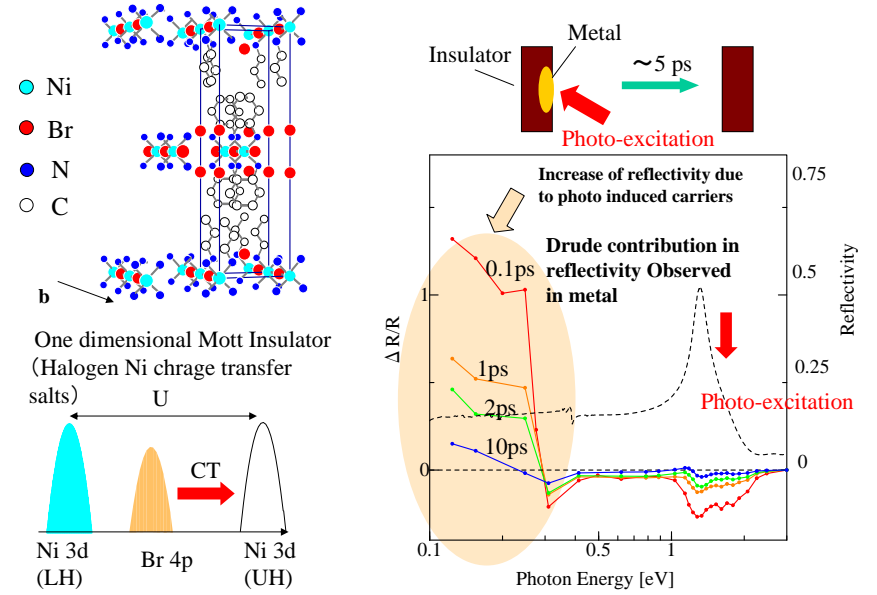


Photo-induced insulator – metal transition

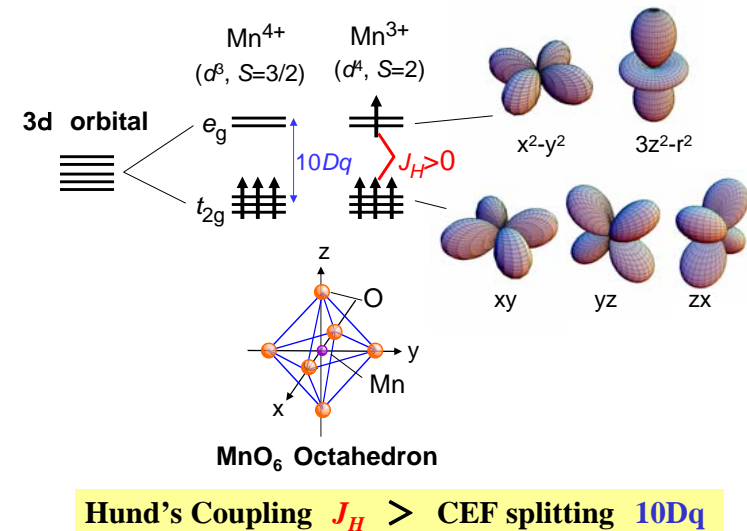


第8図 Pr_{1-x}Ca_xMnO₃ ($x=0.3$) 結晶のナノ秒パルス光励起に伴う光誘起金属化.

Ultra-fast Switching Phenomenon in Strongly Correlated One Dimensional Mott Insulators - Photo Induced Carrier Doping -

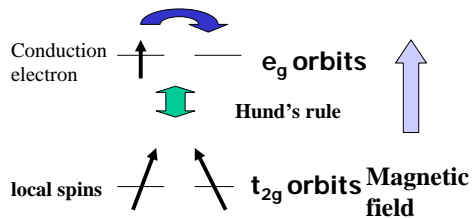


Electronic Structure of Manganese oxides

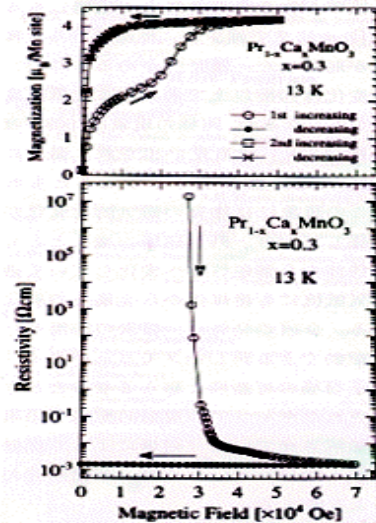


Magnetic Field Control of Magnetic and Transport Properties in $\text{Pr}_{1-x}\text{Ca}_x\text{MnO}_3$

Competition between Ferromagnetic Metallic and charge ordered insulating phases



Conductivity controlled by Magnetic field \rightarrow local spins \rightarrow mobile electrons

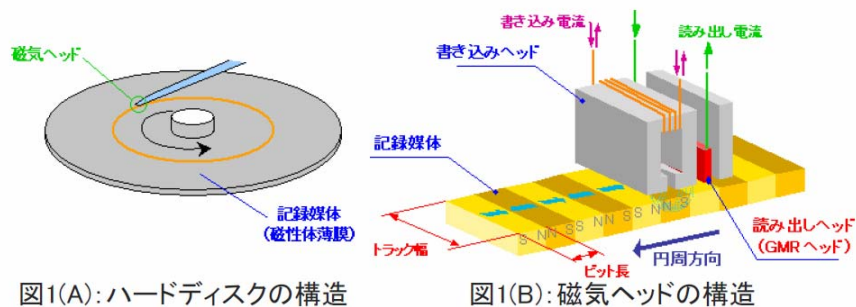
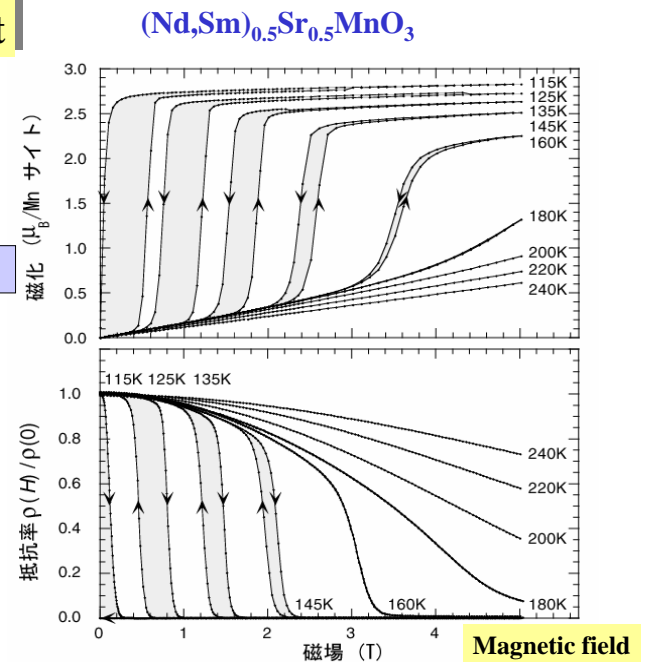


CMR effect

Colossal Magneto Resistance

Magnetization

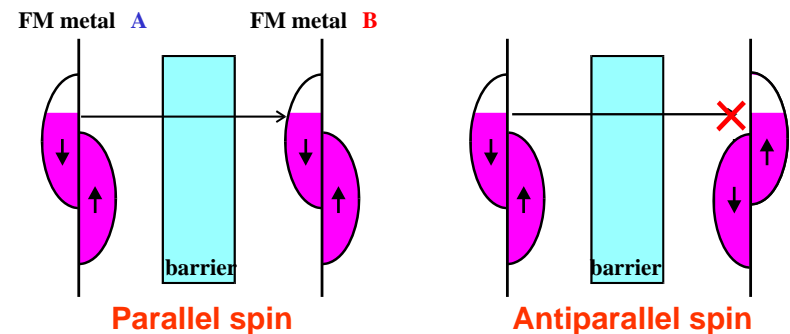
Resistance

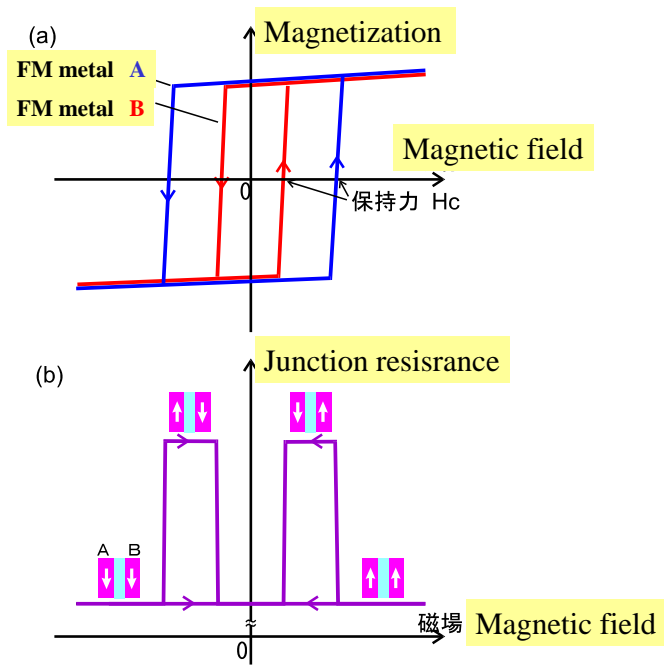


Spin polarization and Tunnel Magneto-Resistance (TMR)

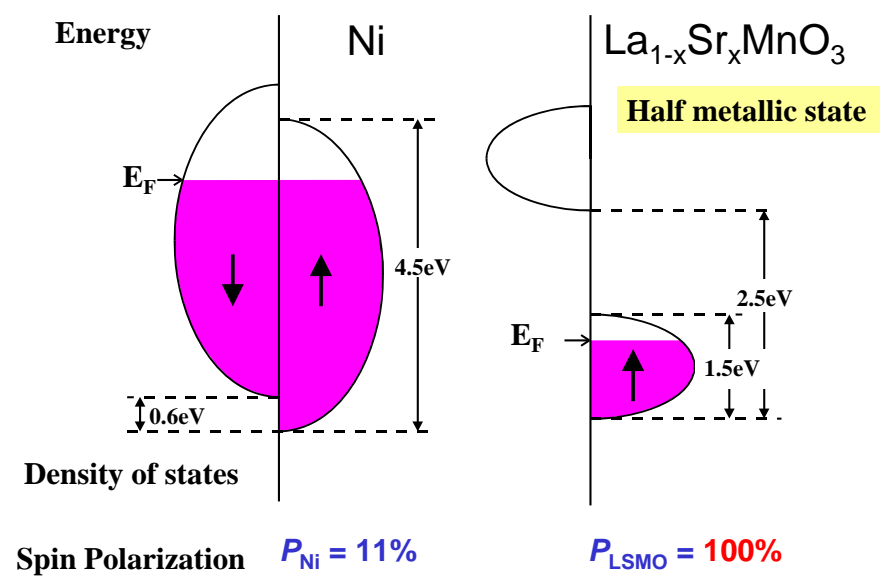
$$\text{TMR} = \frac{\rho_{AF} - \rho_F}{\rho_F} = \frac{2P_A P_B}{1 - P_A P_B} \quad (P_A: \text{spin polarization of metal A})$$

If $P_A = P_B = 1$, then $\text{TMR} \rightarrow \infty$



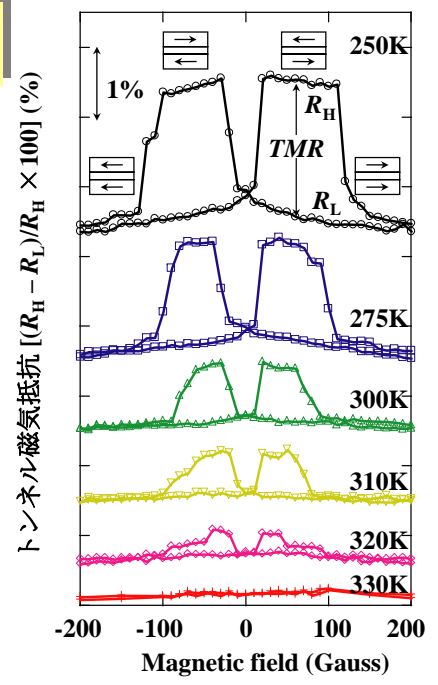


Strong coupling of spin and charge degrees of freedom

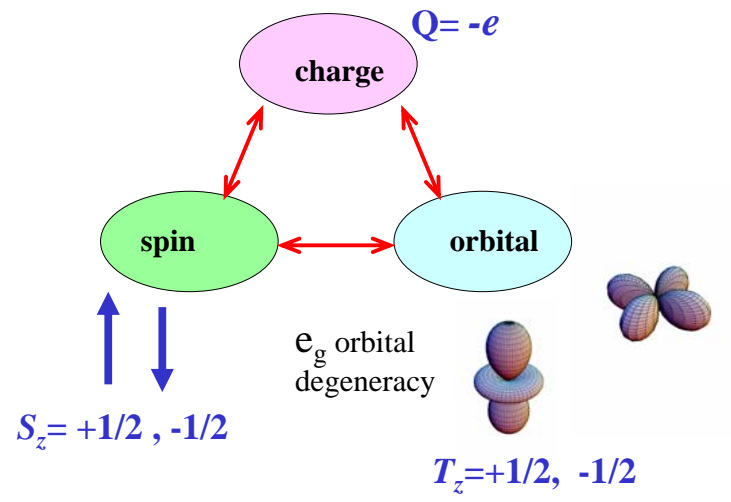


Tunnel Magneto-Resistance (TMR) at room temperature

LSMO/STO/LSMO Junction



Rich electron phases due to three degrees of freedom in strongly correlated matters



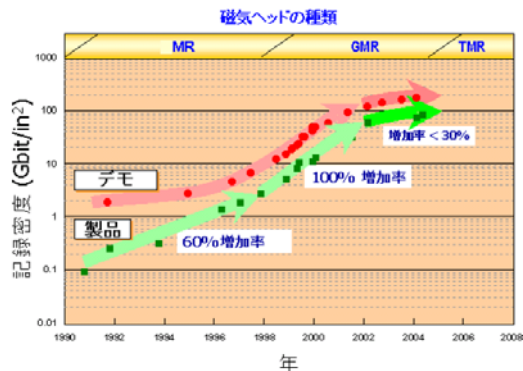
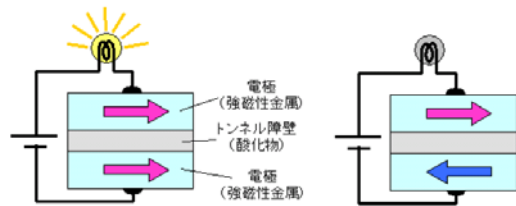


図2: ハードディスクの記録密度の歴史



$$\text{磁気抵抗比} = (R_A - R_P) \div R_P$$

図3: TMR素子のトンネル磁気抵抗(TMR)効果

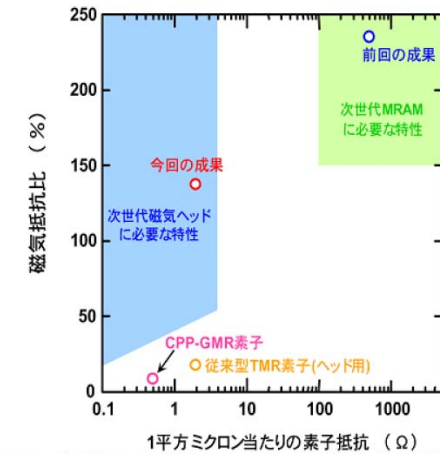


図4: 次世代の磁気ヘッドに要求される特性

Electric-field control of ferromagnetism

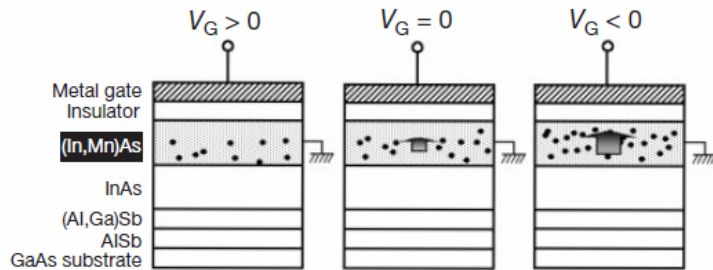


Figure 1 Field-effect control of the hole-induced ferromagnetism in magnetic semiconductor (In,Mn)As field-effect transistors. Shown are the cross-sections of a metal-insulator–semiconductor structure under gate biases V_G . This controls the hole concentration in the magnetic semiconductor channel (filled circles). Negative V_G increases hole concentration, resulting in enhancement of the ferromagnetic interaction among magnetic Mn ions, whereas positive V_G has an opposite effect. The arrow schematically shows the magnitude of the Mn magnetization. The InAs/(Al,Ga)Sb/AISb structure under the (In,Mn)As layer serves as a buffer relaxing the lattice mismatch between the structure and the GaAs substrate to produce a smooth surface on which the magnetic layer is grown.

$$R_{\text{Hall}} = \frac{R_0}{d} B + \frac{R_s}{d} M$$

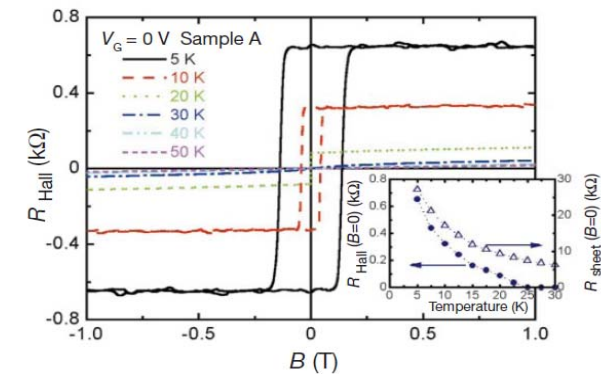


Figure 2 Magnetic-field dependence of the sheet Hall resistance R_{Hall} proportional to the magnetization of the magnetic semiconductor layer. R_{Hall} is used to measure the small magnetization of the channel. Shown are R_{Hall} as a function of field perpendicular to the layer at temperatures $T = 5\text{--}50$ K of sample A at $V_G = 0$ V. Clear hysteresis observed at $T \leq 20$ K is evidence of ferromagnetism. Inset, the temperature dependence of the remanence of R_{Hall} (solid circles), showing that the ferromagnetic transition temperature T_C is above 20 K. Open circles indicate the channel sheet resistance R_{sheet} at zero field, which shows moderate negative T -dependence.

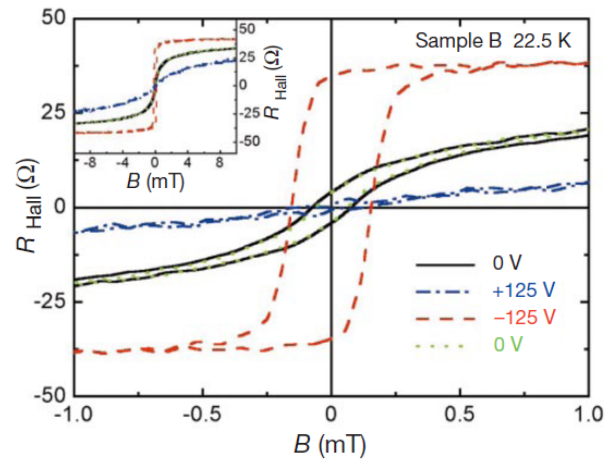


Figure 3 R_{Hall} versus field curves under three different gate biases. Application of $V_G = 0$, $+125$ and -125 V results in qualitatively different field dependence of R_{Hall} measured at 22.5 K (sample B). When holes are partially depleted from the channel ($V_G = +125$ V), a paramagnetic response is observed (blue dash-dotted line), whereas a clear hysteresis at low fields (<0.7 mT) appears as holes are accumulated in the channel ($V_G = -125$ V, red dashed line). Two R_{Hall} curves measured at $V_G = 0$ V before and after application of ± 125 V (black solid line and green dotted line, respectively) are virtually identical. Inset, the same curves shown at higher magnetic fields.

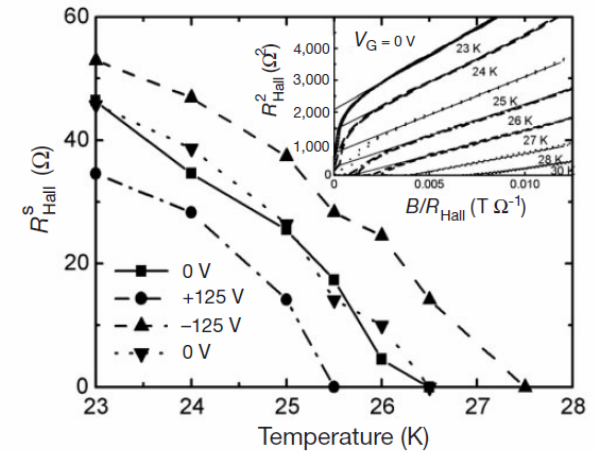


Figure 4 Temperature dependence of spontaneous Hall resistance $R_{\text{Hall}}^{\text{S}}$ under three different gate biases. $R_{\text{Hall}}^{\text{S}}$ proportional to the spontaneous magnetization M_S indicates ± 1 K modulation of T_C upon application of $V_G = \pm 125$ V (sample A). T_C is the temperature at which $R_{\text{Hall}}^{\text{S}}$ (and hence M_S) goes to zero. Data at $V_G = 0$ V before and after application of ± 125 V are shown by squares and down triangles, respectively. In order to minimize the effect of domain rotation and magnetic anisotropy, $R_{\text{Hall}}^{\text{S}}$ is determined by extrapolation of R_{Hall} from moderate fields (0.1–0.7 T) to 0 using Arrott plots (R_{Hall}^2 versus B/R_{Hall} plots shown in inset).

Magnetism on Report (deal line: 11/11)

Read the reference;

H. Ohno, D. Chiba, F. Matsukura, T. Omiya, E. Abe, T. Dietl, Y. Ohno, and K. Ohtani, “Electric-field control of ferromagnetism”, *Nature* 408, 944 (2000).

1. Describe the origin of ferromagnetism in Mn-doped semiconductors.
2. Consider why the decrease (increase) of the hole concentration by the application of electric field results in a reduction (an increase) of hole-mediated ferromagnetic exchange interaction among localized Mn spins.